Kavei G.

NOVEL METHOD FOR POWER GENERATION FROM WASTE HEAT VIA THERMOELECTRIC FOAM

Kavei G.
(Material and Energy Research Centre, P.O. Box 14155-4777, Tehran, 11369, Iran)

- *Thermoelectric modules with the bulk elements are mostly designed to extract waste heat from a hot medium. Heat, in particular, waste heat, is extracted from the surfaces of solid bodies or gaseous media. Thermoelectric modules as a thermocouple (p- and n- types) are typically designed from the bulk thermoelectric elements sandwiched between two flat ceramic plates. New developed open and close porous foam structures are a promising design of thermoelectric modules for conversion of waste heat from the hot bulk surface or gaseous media sources. Foam structure, due to large porosity and high surface area as compared to its bulk counterpart, could be foreseen as an efficient solution to extract the waste heat. Thermoelectric foams have been designed, fabricated and characterized. Porous foams were fabricated as replicas of the $(Bi_{0.25}Sb_{0.75})_2Te_3$ and domestic salt powder at different temperatures synthesized in a hot die pressing system. Raw materials were prepared by mechanical alloying and the formations were characterized by Differential Temperature Analysis, X-Ray diffraction, scanning electron microscopy and particle sizes classification of the powders. The Seebeck coefficient, electrical conductivity, relative density and thermal conductivity of foams were measured or evaluated by empirical assessment.*

Introduction

The manufacturing of thermoelectric (TE) modules from conventional materials is well established and widely commercially available [1]. However, fabrication of modules based on foam materials has been recently emerging and there exist very few reports on their performance. The foam nature of the TE elements and the processing specifications involving ambient temperatures make the fabrication a difficult task and different from that of conventional TE modules. In this work we describe (i) the fabrication of TE modules based on bismuth telluride and foam materials of $(Bi_{0.25}Sb_{0.75})_2Te_3$ and (ii) salt as an item of replicated raw material. Porous foam structures make it possible to design efficient TE modules for waste heat sources involving gaseous media. Large area physical contact of TE foam elements with hot media will make them efficient electric power generators [2].

However, porous TE materials are good candidates to confine phonons (lattice vibrations) in order to reduce the thermal conductivity, if the pores are made sufficiently small. Characteristics of modules are evaluated and possible factors limiting their theoretical performance are discussed [3]. A parameter representing the quality of the modules termed the manufacturing factor representing the cumulative effect of various factors involved in the fabrication process is introduced; the modules are evaluated and compared to other reported modules.

Several unusual behaviors in both the electronic and thermal transport properties of thermodynamically stable systems have been reported significantly contributing to verify the condensed matter evolution [4 – 5]. In fact, the temperature dependence of the electrical conductivity [6], the Seebeck coefficient [7] and the thermal conductivity [8 – 9] strongly suggest that alloys should be properly located at the border line between metals and semiconductors [10]. Searching for novel high TE materials is a challenge [11]. The efficiency of TE devices depends on the transport

coefficients of the constituent materials, and it can be properly expressed in terms of time dependent figure of merit given by the dimensionless expression:

$$\theta \equiv ZT = \frac{T\sigma\alpha^2}{\kappa_e + \kappa_{ph}}, \quad (1)$$

where T is the temperature, σ is the electrical conductivity, α is the Seebeck coefficient and κ_e and κ_{ph} give the contribution to the thermal conductivity due to the electrons and lattice phonons, respectively. Then the appealing question arises regarding whether the irregularity in the transport properties may be properly balanced in Eq. (1) to obtain promising stoichiometry for TE applications. Such a possibility has been recently discussed in the literature from the standpoint of a number of experimental results [12].

Experimental

Bi (99.999 %,), *Te* (99.999 %,) and *Sb* (99.999 %) purity were prepared as starting materials, [13]. The degree of purity and the chemical elemental analysis were evaluated by Inductively Coupled Plasma-Mass-Atomic Emission Spectrophotometer (ICP-AES model ARL 3410+). Atomic Absorption Spectroscopy (AAS) analysis revealed that there were fractions of undesired elements in the samples. Analyses were made on several elements (*Cu*, *Fe*, *Ni*, *Pb* and *S*) by using Graphite Furnace (932 plus, GBC) detection.

Powders were weighted in the stoichiometric proportion of $(Bi_{0.25}Sb_{0.75})_2Te_3$ and then were charged into a stainless steel cup (125 ml) with the ball to powder weight ratio of 10:1. Five high-chromium-stainless steel balls with the diameter of 20 mm were used in the argon atmosphere with the pressure of 3 atm. The ball milling experiments were performed in a planetary ball mill at the cup and main disk speed of 275 and 525 rpm, respectively, for 5, 10 and 15 hours. The samples were removed by interrupting the ball mill at various intervals for analysis. The alloy powder to a particle size ratio of [64 % with the mesh 80 (200 μm^2)/36 % and with the mesh 60 (250 μm^2)] was obtained.

Domestic salt (sodium chloride *NaCl* with 150 – 212 μm powder particle size and 99.0 % purity) was selected as an item of replicated raw material. Sodium chloride was ball-milled in a planetary ball-mill with stainless steel cup for 20 h. Ball-milling was performed at a cup speed of 270 rpm. The balls in a ball miller sphere of 17 mm diameter and the ratio of balls to powder weights is 10:1. Crystallite sizes may be evaluated by using four different methods [14 – 15]. Particles sizes of the resulting pile of powder were measured by "Fritsch GmbH analysette 22" system. The particles sizes population above 30 % for *NaCl* was 4 – 8 μm.

The densities of *NaCl* and $(Bi_{0.25}Sb_{0.75})_2Te_3$ are 2.17 and 6.80 $g \cdot cm^{-3}$, respectively [16]. These have been designated to calculate the relative weights of TE material / *NaCl* and attain the defined porosities. Thermoelectric foam was processed with mixed milled mechanically alloyed powder and *NaCl* powders. The ratio of 2.04 / 1.52 weights of TE material / *NaCl* was calculated to obtain TE foam with a relative porosity of 70 % (see Table 1). The relative porosity is not only changed by adjusting the relative weights of TM / *NaCl* but also one may do it by varying the elementary materials particle size [2].

Mixed mechanically alloyed powder and salt with volume of 1 cm^3 in different ratios of TE material / *NaCl* (see Table 1) were pressed under 500 MPa compressive pressure stress in a steel mold while it is hot. Samples of closed-cell foams to the size of 5 × 10 × 20 mm^3 were formed. Quasi-static uniaxial compression was exerted onto a cross section of 5 × 20 mm. So, the force direction (longitudinal direction) was introduced along 10 mm length on all samples within a displacement-controlled hydraulic load frame. All the tests were carried out in the longitudinal and transverse directions. Longitudinal and transverse directions refer to all those directions that are parallel and perpendicular to a direction in which a sample is pressed, respectively. Hot-pressing was performed at

different temperatures of 300, 400 and 500 °C under a pressure of 500 MPa in argon atmosphere for a period of one minute. Compression was repeated for several times at either temperature to reach a high degree of compact. Such a slow rate of sintering avoids internal stress and micro cracks which leads to perfect compact crystallites (surface to core). Density of the samples at each stage of hot pressing was measured. This procedure stops foam decomposition whilst removing salt from foam. Foam properties largely depend on pressing time [2]. For the present study, a press system cannot be kept under a load for a long time. However, malfunctioning of a press system prevents us from checking time effects.

Table 1

Attainable porosities from theoretical and practical aspects in a certain experimental configuration at T = 300°C

Experiment							Theory			
Material relative porosity	$(Bi_{0.25}Sb_{0.75})_2Te_3$	*NaCl*	Relative porosity	Relative density	Foam weight	*NaCl residue*	Theoretical relative density	$(Bi_{0.25}Sb_{0.75})_2Te_3$	*NaCl*	Size
63% Ref.	2.516	0.0684	62%	38%	2.5844	5%	37%	2.516	1.3671	1 cm^3
65%	2.38	0.1128	64%	367%	2.4928	8%	35%	2.38	1.41	1 cm^3
70%	2.04	0.076	69%	31%	2.116	5%	30%	2.04	1.52	1 cm^3
75%	1.7	0.0813	74%	26%	1.7814	5%	25%	1.7	1.63	1 cm^3

Hot-pressed sample was boiled in water for 2 h in an attempt to remove *NaCl* from the raw foam. This allows for pure TE foam to be achieved.

Predetermined relative density of the foams was measured based on the Archimedes experiment by means of a balance system (Mettler-Toledo Model AG285). The relative density of the foam with respect to its bulk counterparts around 30 % has been obtained. A sensible deviation from the real value of relative density indicates that about 5 – 7 % *NaCl* was left into the foam. $(Bi_{0.25}Sb_{0.75})_2Te_3$ powder is chemically stable against compression and any applied heat in the presence of *NaCl* to bind particles, and allowing us to work with a hot pressing system. The pressure and content in the mould are so manipulated that they make it possible to achieve solidly packed samples.

Phase identification of the sintered compacts was examined by *X*-ray diffraction (XRD) [in a Philips *X*'pert-system, (30 kV and 25 mA) diffractometer with CuK_α radiation (λ = 1.5405 Å) with a step size of 0.02 and a time per step of 1 s]. Morphology of sintered material in longitudinal and transverse sections was examined using a scanning electron microscope (SEM) (Cambridege-30S scanning electron microscope (SEM) operating at 25 kV) to identify the formed phases and micrograph of the surfaces.

Performance of the foam structures as TE leg was examined at different sintering temperatures in a simple characterization process of the foam as Fig. 1. The function was optimum for the sample at 500 °C under a pressure of 500 MPa. Circuit configuration, with the Benson torch flame as the heat source, thermocouples and a mille voltmeter as measurement systems, the foam is observed to have an open circuit voltage of 10 mV at 300 °C and applied temperature gradient of 200 °C.

Measuring the Seebeck voltage was carried out, as one end was heated up and the net voltage appeared between the two ends of the leg. The Seebeck voltage was directly measured on the foam, as expressed by [17]. Electrical conductivity was examined by a method that has been recommended by [18]. Since there were large amounts of voids on the surfaces, the electrical contacts for the foams were

made by coating silver paint up to around 2 mm length, on both ends. Thermal conductivity κ of the samples was measured along the longitudinal direction by a device designed in our laboratory [19]. Finally, figure of merit $Z = \alpha^2\sigma/\kappa$ was calculated for sintering temperature ranges as mentioned above.

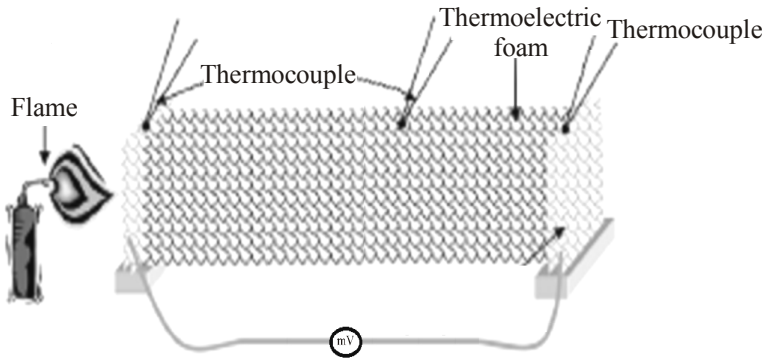

Fig. 1. A simple system for characterization of the foam. The function was optimum for the samples at 500 °C under a pressure of 500 MPa. Circuit configuration is Benson torch flame as the heat source, thermocouples and a mille voltmeter as measurement systems.

Results and Discussion

In order to evaluate the effect of mechanical alloying process on the formation and behavior of the Bi_2Te_3 powder, and then $(Bi_{0.25}Sb_{0.75})_2Te_3$ the prepared Bi_2Te_3 powders at different time intervals were characterized via DTA at a heating rate of 10 °C·min^{-1} in static air. In the as-received sample, the endothermic peak at 270 °C corresponds to the melting of bismuth [20], and the other exothermic peak situated at 418 °C corresponds to the formation of Bi_2Te_3. This is confirmed by the negative enthalpy of the formed Bi_2Te_3 (−119.7 kJ·mol^{-1}) that means the heat released during bismuth and tellurium reaction [20]. Differential thermal analysis (DTA) curves of the as-received (as-mixed) and mechanically alloyed Bi_2Te_3 powders at different time intervals (after 10 h and 5 h of milling) are presented in Fig. 2. At 10 h formation of the compound was entirely observed. Fig. 3 is an illustration of mechanically alloyed powder morphology that has been produced in 10 h of a ball mill. Dense microstructure of the powder grains with more than 30 % particles sizes ranged 20 to 40 μm is evident. Fig. 4 shows morphology from TE foam surface with relative porosity of 70 % at 500 °C hot pressing temperature. In the image, the dense structure as has been created on the surface can be noticed, and the pore size is nearly 2.5 μm.

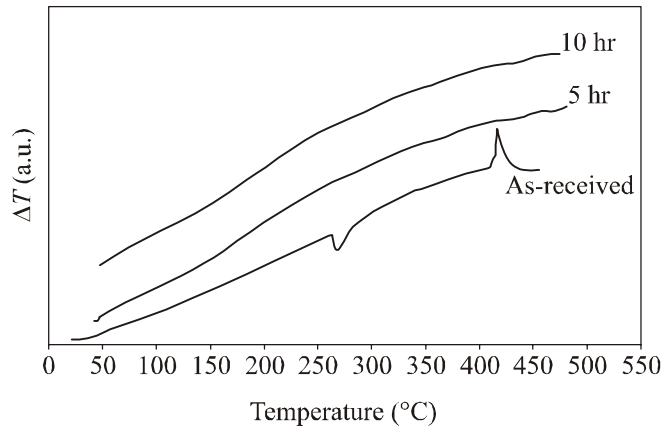

Fig. 2. The differential thermal analysis (DTA) of a typical formation of Bi_2Te_3.

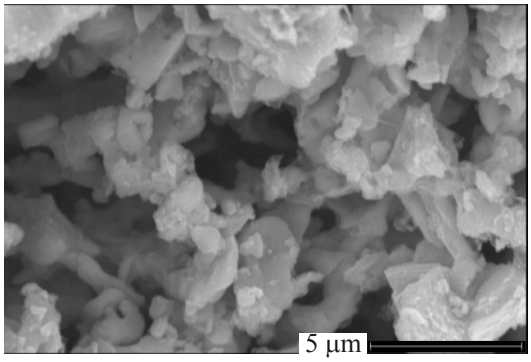

Fig. 3. Mechanically alloyed powder morphology produced in 15 h of ball mill.

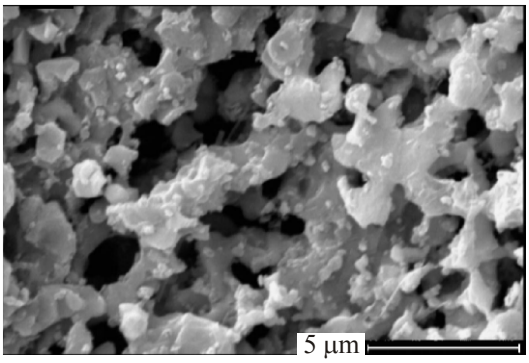

Fig. 4. Morphology from TE foam surface with relative porosity of 70 % at 500 °C hot pressing temperature. The pore size is nearly 2.5 μm.

At this stage, the samples were examined by *X*-ray diffraction diffractometer. Fig. 5 shows XRD pattern from crystallized $(Bi_{0.25}Sb_{0.75})_2Te_3$ foam. All peaks were indexed for the $(Bi_{0.25}Sb_{0.75})_2Te_3$ and *NaCl* phases with no presence of impurities. For the definition of the foam structure in the XRD pattern, it should be noted that the main peaks are available for *NaCl* crystal at 27.5, 31.7, 42.5, 51.5 and 68.5 2θ degrees [21] and for TE material at 17.5, 28, 38, 45 and 57 2θ degrees. Table 2 summarizes the various parameters that were measured at different temperature rates. The table reveals that increasing the hot press temperature results in increment on density and electrical conductivity due to voids expansion and Seebeck coefficient decrement.

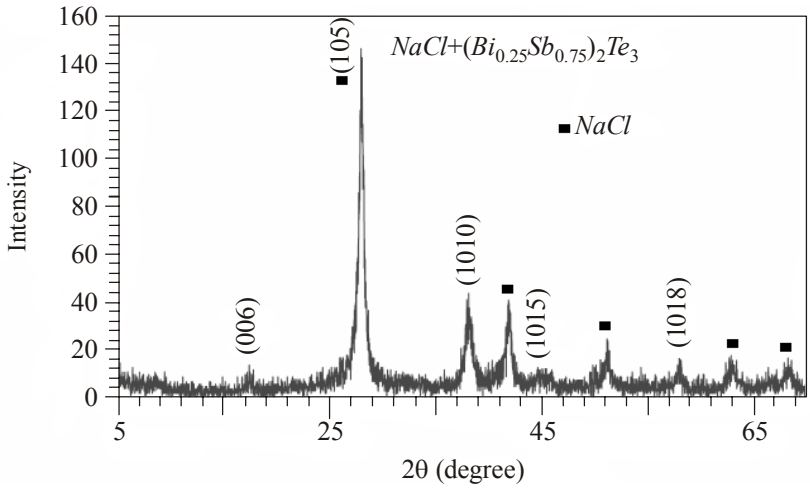

Fig. 5. XRD pattern from crystallized $(Bi_{0.25}Sb_{0.75})_2Te_3$ foam.

Table 2

Various physical parameters measured for the TE foam module at different hot press temperatures

Parameters	T_1 (300 °C)	T_2 (400 °C)	T_3 (500 °C)
A (μV / K)	189	187	186
Σ $(\Omega \cdot cm)^{-1}$	95	106	120
κ $(Wcm^{-1}K^{-1})$	1.3	–	–
ρ / ρ_0 (%)	30	30.5	31

Outlook

As pointed by [22], the pores are assumed to be uniform, and cubes of edge length l are separated by width $2w$. Each cell, then, consists of a cubic space surrounded by a wall of thickness w. For $l \approx 2w$ the electrical and thermal flows are linear. Nevertheless, in an actual foam the pores will be quite different from those in assumed model, but the effect on transport properties is likely valid.

Generally, the thermal conductivity $\kappa_{P,}$ of gas-containing pores will normally be much less than the thermal conductivity κ_s of thermoelectric material. In this case thermal conductance K_C (effective conductivity of the porous material of each cell) is given by (Fu et al., 1998):

$$K_C = \frac{\kappa l}{\kappa / \kappa_p + 2w/l} + \frac{\kappa l[(1+2w/l)^2 - 1]}{1+2w/l}. \quad (2)$$

Effective thermal conductivity is the local volume-averaged thermal conductivity used for the fluid-filled matrices along with the assumption of local thermal equilibrium between the solid and fluid phases. The effective thermal conductivity is not only a function of porosity and the thermal conductivity of each phase, but is very sensitive to the microstructure [23]. Since thermal conductivity of the gas in the pores in comparison with thermoelectric material thermal conductivity was negligible, thermal conductance per cell (K_s conductance of the solid material) would be [24]:

$$K_s = \frac{\kappa l[(1+2w/l)^2 - 1]}{1+2w/l}. \quad (3)$$

where relative thermal conductivity is $K_{Rel} = K_C/K_s$. This is analogous to the ratio of figure of merit Z_p in porous material to Z_o of a fully dense specimen. H.J. Goldsmid calculated this ratio for the voids filled with air, carbon dioxide and krypton. He has showed how the figure of merit falls the same as porosity factor p does in these three instances. The porosity factor p was defined as a ratio of the electrical conductivity in fully dense material to that of porous material. Since the electrical conductivity of gases within the pores is insignificant:

$$p = \frac{(1+2w)^2}{(1+2w)^2 - l^2}. \quad (4)$$

The figure of merit falls down to about 20 % for a porosity factor of 10, if the pores are filled with air and the same 20 % for the same porosity factor which is less than 10 %, if the gas is krypton.

Conclusion

The prospects of foam structures are quite promising. The availability of TE foams could provide designing unique and efficient TE modules, in particular, for specific heat source environments. TE foams are also of interest to replace bulk TE elements in conventional module designs. Foams fabrication from high efficiency thermoelectric materials and the concept of using foam structures to extract waste heats from gaseous environments have been discussed. The high surface area and optimal porosity of 70 % of the foams allows an efficient heat extraction as compared to bulk materials. The thermoelectric $(Bi_{0.25}Sb_{0.75})_2Te_3$ material has been processed as a replica of salt foams and tested as a thermoelectric generator. In a simple thermoelectric module configuration an open circuit voltage of 10 mV was measured at 300 °C and applied temperature gradient of 200 °C.

References

1. B.I. Ismail, W.H. Ahmed TE Power Generation Using Waste-Heat Energy as an Alternative Green Technology, Recent Patents on Electrical Engineering, 2, 27 – 39 (2009).
2. E.S. Reddy, J.G. Noudem, C. Goupil Open Porous Foam Oxide Thermoelectric Elements for Hot

Gases and Liquid Environments, Energy Conversion and Management 48(4), 1251 – 1254 (2007).
3. K. Vafai, Handbook of Porous Media (CRC Press Taylor & Francis Group, USA, 2005).
4. A.P. Tsai, A. Inoue, T. Masumoto, Stable Icosahedral *Al-Pd-Mn* and *Al-Pd-Re* Alloys, Mater. Trans. Jpn. Inst. Metal. 31, 98 – 103 (1990).
5. C. Janot, Conductivity in Quasicrystals via Hierarchically Variable-Range Hopping, Phys. Rev. *B* 53, 181 – 191 (1996).
6. O. Rapp, in: Physical Properties of Quasicrystals, Springer Series in Solid-State Physics, Vol. 126, ed. by Z.M. Stadnik (Springer, Berlin, 1999).
7. F. Giraud, T. Grenet, C. Berger, P. Lindqvist, C. Gignoux, G. Fourcaudot, Resistivity, Hall Effect and Thermopower in *AlPdMn* and *AlCuFe* Quasicrystals, Czech. J. Phys. 46, 2709 – 16 (1999).
8. J.W. Sharp, C.B. Sales, D.G. Mandrus, B.C. Chakoumakos, Thermoelectric Properties of Tl_2SnTe_5 and Tl_2GeTe_5, Appl. Phys. Lett. 74 (25), 3794 – 96 (1999).
9. P.A. Kalugin, M.A. Chernikov, A. Bianchi, H.R. Ott, Structural Scattering of Phonons in Quasicrystals, Phys. Rev. B 53, 14145 – 51 (1996).
10. R. Tamura, A. Waseda, K. Kimura, H. Ino, Semiconductor-like Transport in Highly Ordered *Al-Cu-Ru* Quasicrystals, Phys. Rev. B 50, 9640 – 43 (1994).
11. T.M. Tritt, Thermoelectric Materials: Holey and Unholey Semiconductors, Science 283, 804 – 805 (1999).
12. A.L. Pope, T.M. Tritt, M.A. Chernikov, M. Feuerbacher, Thermal and Electrical Transport Properties of the Single-Phase Quasicrystalline Material: $Al_{70.8}Pd_{20.9}Mn_{8.3}$ Appl. Phys. Lett. 75, 1854 – 1856 (1999).
13. M.A. Karami, M. Sc. Thesis (Material and Energy Research Center, Iran, 2006).
14. H.P. Klug, L. Alexander, *X*-ray Diffraction Procedures for Polycrystalline and Amorphous Materials (John Wiley& Sons, New York, USA, 1974).
15. M. Herrmann, H. Fietzek, Investigation of the Micro Structure of Energetic Crystals by Means of *X*-Ray Powder Diffraction, Advances in *X*-ray Analysis 48, 52 – 58 (2005).
16. David R. Lide, CRC Handbook of Chemistry and Physics 88th ed (2007).
17. A.V. Petrov, V.A. Kutasov, Thermoelectric Properties of Semiconductors (New York, 1964).
18. G.M. Kavei, A. Karami, Fabrication and Characterization of the *p*-type $(Bi_2Te_3)_x(Sb_2Te_3)_{1-x}$ Thermoelectric Crystals Prepared via Zone Melting, Bull. Mater. Sci. 29 (7), 659 – 663 (2006).
19. G. Kavei, Y. Zare, A. Seyyedi, Tentative Designs for Measurements of Absolute Value of Thermal Conductivity of Semi-Conducting Thermoelectric Elements, J.Thermoelectricity 2, 57 – 61 (2008).
20. O. Kubaschewski, Materials Thermochemistry, 6-th ed. (Pergamon Press, Oxford, 1993).
21. J.W. Anthony, R.A. Bideaux., K.W. Bladh, M.C. Nichols, Handbook of Mineralogy (Mineral Data Publishing, Tucson, Arizona, USA, 1990).
22. H.J. Goldsmid, Porous Thermoelectric Materials, Materials 2, 903 – 910 (2009).
23. M. Kaviany, Principles of Heat Transfer in Porous Media (Springer, New York, 1991).
24. A.M. Druma, M.K. Alam, C. Druma, Surface Area and Conductivity of Open-Cell Carbon Foams, Journal of Minerals & Materials Characterization & Engineering 5 (1), 73 – 86 (2006).

Submitted 19.09.2011.